RKHS based State Estimator for Radar Sensor in Indoor Application

Uday Kumar Singh
SnT, University of Luxembourg
University of Luxembourg
Luxembourg, Luxembourg
uday.singh@uni.lu

Mohammad Alaee-Kerahroodi
SnT, University of Luxembourg
University of Luxembourg
Luxembourg, Luxembourg
mohammad.alaee@uni.lu

M. R. Bhavani Shankar
SnT, University of Luxembourg
University of Luxembourg
Luxembourg, Luxembourg
bhavani.shankar@uni.lu

Abstract—For the estimation of targets' states (location, velocity, and acceleration) from nonlinear radar measurements, usually, the improved version of well known Kalman filter: extended Kalman filter (EKF) and unscented Kalman filter (UKF) are used. However, EKF and UKF approximates the nonlinear measurement function either by Jacobian or using sigma points. Consequently, because of the approximation of the measurement function, the EKF and UKF cannot achieve high estimation accuracy. The potential solution is to replace the approximation of nonlinear measurement function with its estimate, obtained in high dimensional reproducing kernel Hilbert space (RKHS). An ample amount of research has been done in this direction, and the combined filter is termed RKHS based Kalman filter. However, there is a shortage of literature dealing with estimating the dynamic state of the target in an indoor environment using RKHS based Kalman filter. Therefore, in this paper, we propose the use of RKHS based Kalman filter for indoor application. Specifically, we validate the suitability of the RKHS based Kalman filtering approach using simulations performed over three different target motion models.

Index Terms—EKF, UKF, RKHS, Jacobain, Kalman

I. INTRODUCTION

In the radar tracking system, the Kalman filter and its advanced versions, the extended Kalman filter (EKF), and, the unscented Kalman filter (UKF), have been used extensively for estimating the states of the moving targets and updating the measurements [1]–[4]. Depending on the underlying target motion model, the modeled/ estimated states include location or velocity or acceleration and combinations thereof. If the measurements from the radar sensor are already the noisy state vectors, the primary Kalman filter is the optimum choice since the states are linearly related to the measurements i.e., the resulting measurement function ($\mathbf{h}$) is linear. However, in practice, the radar sensors report the noisy measurements in the spherical coordinate, composed of the radial range (r), azimuth (θ), and elevation (ϕ). With the measurement in spherical coordinate, $\mathbf{h}$, relating the target's states in 3D space with the radar measurement is nonlinear. Therefore, the basic Kalman filter, which is optimum for linear $\mathbf{h}$, is not suitable.

To address this issue in practical radar sensors used in various tracking applications, EKF and UKF are considered, as they handle the non-linearity in $\mathbf{h}$ better. In the EKF, the $\mathbf{h}$

is approximated by its equivalent Jacobian matrix evaluated at the predicted state vector. Similarly, with UKF, as the name implies, the $\mathbf{h}$ is approximated by the unscented sigma points. Conceptually, both EKF and UKF are based on the approximation of nonlinear measurement function, and this creates a scope of improving the performance of EKF and UKF by replacing the approximation of $\mathbf{h}$ with its efficient estimate ($\hat{\mathbf{h}}$).

In the light of the above discussion, since Kalman filtering is an iterative technique, the estimate of $\mathbf{h}$ can also be obtained iteratively by the nonlinear adaptive filtering techniques based on reproducing kernel Hilbert space (RKHS). The RKHS based techniques are successfully applied in many nonlinear signal processing, radar, and communication applications [5]–[8]. The idea of combining the utilities of Kalman filtering and RKHS based techniques is initially pursued in [9], [10]. For instance, in [9], a specific time series prediction problem is solved utilizing RKHS based Kalman filter. Subsequently, in [10], RKHS based kernel recursive least square (KRLS) algorithm is used in conjunction with EKF under the assumption that only radial range and the slope are available as the sensor measurement; however, this assumption is infeasible in practice. Despite an ample amount of theoretical work done in [9], [10], the existing literature lacks a thorough analysis of the proposed technique for various practical target motion models. The indoor environment is a case in point, where the slow (around 2 m/sec) and the target's random movement (especially acceleration) make the state prediction problem challenging. The situation becomes more challenging when the measurements from the sensors are available in spherical coordinates, i.e., (r, θ, ϕ). Therefore, this paper aims to investigate the utility of combining EKF and KRLS in such situations. Further, in the line of the research pursued in [9], [10], the main contributions of the paper are:

- We propose the use of the KRLS algorithm to estimate $\mathbf{h}$ and use it with EKF for evaluating states of the target moving in an indoor environment [10]. The states estimation is done using the sensor measurements available in spherical coordinates. The resulting combined filter (EKF plus RKHS based KRLS) is termed EKF-RKHS.
- With the help of various target motion models (constant

displacement, constant velocity, and constant acceleration), we validate the improved performance of EKF-RKHS over conventional EKF. Although we have shown the enhanced performance of EKF-RKHS for all three models, EKF-RKHS is most primarily useful for the constant acceleration model.

- Unlike EKF, in EKF-RKHS, as $\mathbf{h}$ is estimated in terms of the hidden state vector, the EKF-RKHS could be readily deployable in the applications where $\mathbf{h}$ is unknown.

The rest of the paper is organized as follows. The basic problem formulation is described in Section II. Next, in Section III, the proposed approach of using EKF-RKHS for the target state estimation problem is described in detail. Further, in section IV, simulations are performed over the practical target motion model and comparative conclusions are drawn between classical EKF and EKF-RKHS. Lastly, conclusions are drawn in Section V.

Notations: Scalar variables (constants) are denoted by lower (upper) case letters. Vectors (matrices) are denoted by bold face lower (upper) case letters. Superscripts $(.)^T$, $(.)^H$ and $(.)^*$ denote matrix/vector transpose, complex conjugate transpose and scalar complex conjugation operation respectively. $\mathbb{E}[.]$ denotes statistical expectation and $\mathbb{R}$ denote the set of real numbers. $\mathbf{I}_n$ denotes the identity matrix of cardinality n.

II. PROBLEM FORMULATION

Let the evolution of target state vector with cardinality n_s ($\mathbf{s}_k \in \mathbb{R}^{n_s \times 1}$) at any arbitrary time instance k be given by

$$\mathbf{s}_k = \mathbf{f}(\mathbf{s}_{k-1}) + \mathbf{w}_k, \tag{1}$$

where, $\mathbf{s}_{k-1}$ is the previous target state vector, $\mathbf{f}(\cdot) \in \mathbb{R}^{n_s \times 1}$ governs the motion of the target, and $\mathbf{w}_k \in \mathbb{R}^{n_s \times 1}$, accounts for uncertainties in the modelling of the state model. In this work, $\mathbf{w}_k$, is assumed to be Gaussian distributed with zero mean and known covariance $\mathbf{Q}_s = \mathbb{E}[\mathbf{w}_k \mathbf{w}_k^T]$, s.t. $\mathbf{w}_k \sim \mathcal{N}_{\mathbb{R}}(0, \mathbf{Q}_s)$.

Corresponding to (1), the sensor measurements with cardinality n_m at k^{th} time instance ($\mathbf{y}_k \in \mathbb{R}^{n_m \times 1}$) are given by

$$\mathbf{y}_k = \mathbf{h}(\mathbf{s}_k) + \mathbf{v}_k, \tag{2}$$

where, $\mathbf{h}(\cdot) \in \mathbb{R}$ is the nonlinear measurement function and $\mathbf{v}_k \in \mathbb{R}^{n_m \times 1}$ accounts for the error in estimating $\mathbf{y}_k$ using radar sensor. In this work, $\mathbf{v}_k$, is assumed to be Gaussian distributed with zero mean and known covariance $\mathbf{R}_m = \mathbb{E}[\mathbf{v}_k \mathbf{v}_k^T]$, s.t. $\mathbf{v}_k \sim \mathcal{N}_{\mathbb{R}}(0, \mathbf{R_m})$.

In (1), the components of $\mathbf{s}_k$ depend on the type of target motion model. In this work, to analyze the performance of EKF and EKF-RKHS, three different practical target motion models are considered. The associated $\mathbf{f}(\mathbf{s}_{k-1})$ for these three different target motion model are given by [4]:

1) *Constant displacement*: The target state vector is composed of varying target location in 3D space i.e. $\mathbf{s}_k = [x_k, y_k, z_k]^T$ and at each k time instance $\mathbf{s}_k$ is incremented by the constant factor Δs. Consequently, the noise-free $\mathbf{f}(\mathbf{s}_{k-1})$ is given by

$$\mathbf{f}(\mathbf{s}_{k-1}) = \mathbf{s}_{k-1} + \Delta s. \tag{3}$$

2) *Constant velocity*: In this classical setting, the target state vector is composed of dynamic target location in 3D space and the corresponding constant velocities (v_{xk}, v_{yk}, v_{zk}) along x, y, and z axis i.e. $\mathbf{s}_k = [x_k, v_{xk}, y_k, v_{yk}, z_k, v_{zk}]^T$. Hence, the noise-free $\mathbf{f}(\mathbf{s}_{k-1})$ is given by

$$\mathbf{f}(\mathbf{s}_{k-1}) = \begin{bmatrix} 1 & T_{\text{cpi}} & 0 & 0 & 0 & 0 \\ 0 & 1 & 0 & 0 & 0 & 0 \\ 0 & 0 & 1 & T_{\text{cpi}} & 0 & 0 \\ 0 & 0 & 0 & 1 & 0 & 0 \\ 0 & 0 & 0 & 0 & 1 & T_{\text{cpi}} \\ 0 & 0 & 0 & 0 & 0 & 1 \end{bmatrix} \mathbf{s}_{k-1}. \tag{4}$$

where T_{cpi} is the coherent pulse interval (CPI) of the radar sensor. It should be worth mentioning that the constant velocity and constant displacement model similarly evolve the target locations. However, the two models differ in the content of $\mathbf{s}_k$. Consequently, the constant velocity model gives more information about the target's states.

3) *Constant acceleration*: In this refined model, the target state vector is composed of target location in 3D space, corresponding varying velocities (v_{xk}, v_{yk}, v_{zk}) and the constant accelerations (a_{xk}, a_{yk}, a_{zk}) along x, y, and z axis i.e. $\mathbf{s}_k = [x_k, v_{xk}, a_{xk}, y_k, v_{yk}, a_{yk}, z_k, v_{zk}, a_{zk}]^T$. Therefore, the noise-free $\mathbf{f}(\mathbf{s}_{k-1})$ is given by

$$\mathbf{f}(\mathbf{s}_{k-1}) = \tag{5}$$

$$\begin{bmatrix} 1 & T_{\text{cpi}} & 0.5T_{\text{cpi}}^2 & 0 & 0 & 0 & 0 & 0 & 0 \\ 0 & 1 & T_{\text{cpi}} & 0 & 0 & 0 & 0 & 0 & 0 \\ 0 & 0 & 1 & 0 & 0 & 0 & 0 & 0 & 0 \\ 0 & 0 & 0 & 1 & T_{\text{cpi}} & 0.5T_{\text{cpi}}^2 & 0 & 0 & 0 \\ 0 & 0 & 0 & 0 & 1 & T_{\text{cpi}} & 0 & 0 & 0 \\ 0 & 0 & 0 & 0 & 0 & 1 & 0 & 0 & 0 \\ 0 & 0 & 0 & 0 & 0 & 0 & 1 & T_{\text{cpi}} & 0.5T_{\text{cpi}}^2 \\ 0 & 0 & 0 & 0 & 0 & 0 & 0 & 1 & T_{\text{cpi}} \\ 0 & 0 & 0 & 0 & 0 & 0 & 0 & 0 & 1 \end{bmatrix} \mathbf{s}_{k-1}.$$

The primary objective of this work is to effectively and accurately estimate the hidden state vector $(\mathbf{s}_k)$ from $\mathbf{y}_k$ for the three aforementioned motion models.

III. PROPOSED APPROACH

In this section, the proposed approach of using EKF-RKHS to estimate the $(\mathbf{s}_k)$ is described in detail. Firstly, a brief description of the EKF is given, followed by the implementation of EKF-RKHS.

A. EKF

For the state and measurement model described respectively in (1) and (2), let at k^{th} time instance, the available estimate of $\mathbf{s}_{k-1}$ be $\hat{\mathbf{s}}_{k-1}$ and the corresponding error covariance matrix is $\mathbf{P}_{k-1} = \mathbb{E}[(\mathbf{s}_{k-1} - \hat{\mathbf{s}}_{k-1})(\mathbf{s}_{k-1} - \hat{\mathbf{s}}_{k-1})^T]$. The EKF propagates $\hat{\mathbf{s}}_{k-1}$ and $\mathbf{P}_{k-1}$ iteratively and yield the final estimate of $\mathbf{s}_k$ in

two steps a) prediction and b) update. In prediction step, the EKF, predicts $\mathbf{s}_k$ and $\mathbf{P}_k$ with the help of following equations:

$$\mathbf{s}_k^p = \mathbf{F}_{k-1}\hat{\mathbf{s}}_{k-1},$$
$$\mathbf{P}_k^p = \mathbf{F}_{k-1}\mathbf{P}_{k-1}\mathbf{F}_{k-1}^T + \mathbf{Q}_s, \qquad (6)$$

where $\mathbf{F}_{k-1} \in \mathbb{R}^{n_s \times n_s}$ is the motion model matrix and can be obtained respectively from (3), (4), or (5), depending upon the motion model.

After prediction, in the update step, the predictions made in (6) are updated with the help of available measurement from radar sensor ($\mathbf{y}_k$). The following equations give the update equations of EKF:

$$\mathbf{y}_k^p = \mathbf{H}_k\mathbf{s}_k^p, \qquad (7)$$
$$\mathbf{K}_k = \mathbf{P}_k^p\mathbf{H}_k^T(\mathbf{H}_k\mathbf{P}_k^p\mathbf{H}_k^T + \mathbf{R}_m)^{-1},$$
$$\hat{\mathbf{s}}_k = \mathbf{s}_k^p + \mathbf{K}_k(\mathbf{y}_k - \mathbf{y}_k^p),$$
$$\mathbf{P}_k = \mathbf{P}_k^p - \mathbf{K}_k\mathbf{H}_k\mathbf{P}_k^p.$$

where $\mathbf{H}_k = \left.\frac{\partial \mathbf{h}(\mathbf{s}_k)}{\partial \mathbf{s}_k}\right|_{\mathbf{s}_k = \mathbf{s}_k^p} \in \mathbb{R}^{n_m \times n_s}$ is the Jacobain matrix of $\mathbf{h}$ (evaluated at prediction $\mathbf{s}_k^p$), $\mathbf{y}_k^p$ is the predicted measurement, $\mathbf{K}_k$ is the Kalman gain, and $\hat{\mathbf{s}}_k$ and $\mathbf{P}_k$ are the final estimate of $\mathbf{s}_k$ and updated error covaraince matrix, respectively.

From (7), it is explicit that EKF linearizes $\mathbf{h}$ via Jacobian, which yields the first-order approximation of $\mathbf{h}$. Consequently, it restricts EKF from achieving the high estimation accuracy and, in some cases, yielding inaccurate results. Also, to obtain the Jacobian, and hence, to implement the further steps, EKF is bound to know the exact form of $\mathbf{h}$ (which depends on the radar sensor type and, in most cases, not known apriori). In the following subsection, we present an approach to deal with these shortcomings in EKF. We describe the implementation of RKHS based EKF (EKF-RKHS), which first estimates the $\mathbf{h}$ in RKHS using a well-known RKHS algorithm (KRLS). Subsequently, the estimate of $\mathbf{h}$ is plugged in EKF for performing further prediction and update.

The advantages of using EKF-RKHS over EKF are two fold: (1) Unlike EKF, the implementation of EKF-RKHS is not restricted to knowing the exact form of $\mathbf{h}$. (2) Since, unlike EKF, the estimate of $\mathbf{h}$ is used, the EKF-RKHS will yield the estimate of $\mathbf{s}_k$ with higher accuracy.

B. EKF-RKHS

In this subsection, the description of KRLS algorithm used in the implementation of EKF-RKHS, is provided. Firstly, referring to (2), the hidden state $\mathbf{s}_k$ is mapped to a high dimensional RKHS ($\mathcal{H}$) via an unknown implicit mapping function $\phi(\cdot)$. Subsequently, the estimate of $\mathbf{y}_k$ in $\mathcal{H}$ is given by the well known Representer's theorem [11] as

$$\hat{\mathbf{y}}_k = \langle \boldsymbol{\omega}, \phi(\mathbf{s}_k)\rangle_{\mathcal{H}}, \qquad (8)$$

where $\langle (\cdot, \cdot)\rangle_{\mathcal{H}}$ is the inner product in $\mathcal{H}$ and $\boldsymbol{\omega}$ is the unknown weight vector in $\mathcal{H}$.

In the search of the optimized value of $\boldsymbol{\omega}$ and for the available pair of $\mathbf{y}_k$ and $\mathbf{s}_k$, $\{(\mathbf{s}_0, \mathbf{y}_0), \ldots, (\mathbf{s}_{k-1}, \mathbf{y}_{k-1})\}$, the KRLS algorithm minimizes the following cost function

$$\mathcal{J}(\boldsymbol{\omega}) = \min_{\boldsymbol{\omega}} \sum_{j=0}^{k-1} |\mathbf{y}_j - \hat{\mathbf{y}}_j|^2 + \lambda \|\boldsymbol{\omega}\|^2, \qquad (9)$$

where λ is the regularization factor.

Utilizing (8), yields

$$\mathcal{J}(\boldsymbol{\omega}) = \min_{\boldsymbol{\omega}} \sum_{j=0}^{k-1} |\mathbf{y}_j - \langle \boldsymbol{\omega}, \phi(\mathbf{s}_j)\rangle_{\mathcal{H}}|^2 + \lambda \|\boldsymbol{\omega}\|^2, \qquad (10)$$

The detailed steps of solving (10) is given in [12]. After solving (10), $\boldsymbol{\omega}$ is given by

$$\boldsymbol{\omega} = \sum_{j=0}^{k-1} a_j \phi(\mathbf{s}_j) = \mathbf{a}_{k-1}\boldsymbol{\Phi}_{k-1}, \qquad (11)$$

where $\mathbf{a}_{k-1} = [a_0, \ldots, a_{k-1}]$ and $\boldsymbol{\Phi}_{k-1} = [\phi(\mathbf{s}_0), \ldots, \phi(\mathbf{s}_{k-1})]^T$. Substituting (11) in (8), yields

$$\hat{\mathbf{y}}_k = [\langle \phi(\mathbf{s}_0), \phi(\mathbf{s}_k)\rangle_{\mathcal{H}}, \ldots, \langle \phi(\mathbf{s}_{k-1}), \phi(\mathbf{s}_k)\rangle_{\mathcal{H}}]\mathbf{a}_{k-1}^T. \quad (12)$$

From (12), we can readily analyze that the estimate of $\mathbf{h}$ at k^{th} time instant is given by

$$\hat{\mathbf{h}}_k = [\langle \phi(\mathbf{s}_0), \phi(\mathbf{s}_k)\rangle_{\mathcal{H}}, \ldots, \langle \phi(\mathbf{s}_{k-1}), \phi(\mathbf{s}_k)\rangle_{\mathcal{H}}]. \qquad (13)$$

For simplifying (12), we use the Mercer's theorem [5], which states that the inner product between any two functions $\{\phi(\mathbf{s}_i), \phi(\mathbf{s}_j)\}$ in $\mathcal{H}$ can be equivalently evaluated in Euclidean space by using a reproducing kernel $\kappa(\cdot, \cdot)$ as

$$\kappa(\mathbf{s}_i, \mathbf{s}_j) = \langle \phi(\mathbf{s}_i), \phi(\mathbf{s}_j)\rangle_{\mathcal{H}},$$

Hence, utilizing the Mercer's theorem, the simplified form of $\hat{\mathbf{h}}_k$ is given by

$$\hat{\mathbf{h}}_k = [\kappa(\mathbf{s}_0, \mathbf{s}_k), \ldots, \kappa(\mathbf{s}_{k-1}, \mathbf{s}_k)]. \qquad (14)$$

Form (14), we can draw an inference that $\mathbf{h}$ is estimated iteratively, and at k^{th} instant, the estimate is based on the present state vector $\mathbf{s}_k$ and the past state vectors $\{\mathbf{s}_0, \ldots, \mathbf{s}_{k-1}\}$. This implies that at k^{th} time instant after obtaining $\hat{\mathbf{s}}_k$ from EKF, in (14), the $\hat{\mathbf{s}}_k$ replaces $\mathbf{s}_k$. Afterwards, $\hat{\mathbf{h}}_k$ replaces $\mathbf{h}$ in EKF to do the further prediction and update steps. Henceforth, the process repeats iteratively for $k = 1, 2, \ldots, K$. The pseudo algorithm for EKF-RKHS is given in Algorithm 1, where $\mathbf{z}_k$, r_k, $\mathbf{Q}_k$, $\mathbf{e}_k$, and $\mathbf{a}_k$ are as per [12].

IV. SIMULATION RESULTS AND INFERENCE

In this section, a thorough analysis of simulation results performed over target motion models described in Section II is provided. The performance of both EKF and EKF-RKHS are simulated for $K = 200$ time instances. The three target motion models: constant displacement, constant velocity, and constant acceleration, are respectively termed as the scenario I, scenario II, and scenario III. For all scenarios $T_{\text{cpi}} = 10^{-3}$ sec. The theoretical mean square error (TMSE) is used as a metric

Algorithm 1: Implementation of EKF-RKHS

Intialization:

1 $\mathbf{s}_0, \mathbf{y}(\mathbf{s}_0), \hat{\mathbf{s}}_0, \mathbf{P}_0, \hat{\mathbf{h}}_0 = [\kappa(\hat{\mathbf{s}}_0, \hat{\mathbf{s}}_0)],$
$\mathbf{Q}_0 = (\lambda + \kappa(\hat{\mathbf{s}}_0, \hat{\mathbf{s}}_0))^{-1}, \mathbf{a}_0 = [1, \ldots, 1]^{1 \times n_m}$

2 **for** $k = 1, 2, 3, \cdots, K$ **do**

3   EKF

4   Compute $\mathbf{s}_k^p$ and $\mathbf{P}_k^p$ using (6)

5       $\mathbf{y}_k^p = \mathbf{a}_{k-1}^T \hat{\mathbf{h}}_{k-1}^T$

6       $\hat{\mathbf{H}}_k = \left\{ \left(\frac{\partial \hat{\mathbf{h}}_{k-1}}{\partial \hat{\mathbf{s}}_{k-1}} \bigg|_{\hat{\mathbf{s}}_{k-1}=\mathbf{s}_k^p} \right) \mathbf{a}_{k-1} \right\}^T$

7   Compute $\mathbf{K}_k, \hat{\mathbf{s}}_k,$ and $\mathbf{P}_k$ using (7)

8   KRLS

9       $\mathbf{z}_k = \mathbf{Q}_{k-1} \hat{\mathbf{h}}_{k-1}^T$

10       $r_k = \lambda + \kappa(\hat{\mathbf{s}}_k, \hat{\mathbf{s}}_k) - \mathbf{z}_k^T \hat{\mathbf{h}}_{k-1}^T$

11       $\mathbf{Q}_k = r_k^{-1} \begin{bmatrix} \mathbf{Q}_{k-1} r_k + \mathbf{z}_k \mathbf{z}_k^T & -\mathbf{z}_k \\ -\mathbf{z}_k^T & 1 \end{bmatrix}$

12       $\mathbf{e}_k = \mathbf{y}_k - \mathbf{a}_{k-1}^T \hat{\mathbf{h}}_{k-1}^T$

13       $\mathbf{a}_k = \begin{bmatrix} \mathbf{a}_{k-1} - r_k^{-1} \mathbf{z}_k \mathbf{e}_k^T \\ r_k^{-1} \mathbf{e}_k^T \end{bmatrix}$

14       $\hat{\mathbf{h}}_k = [\kappa(\hat{\mathbf{s}}_0, \hat{\mathbf{s}}_k), \ldots, \kappa(\hat{\mathbf{s}}_{k-1}, \hat{\mathbf{s}}_k)]$

15 **end**

for comparing the performance of EKF and EKF-RKHS. The TMSEs corresponding to the elements of $\hat{\mathbf{s}}_k$ are defined by

$$\text{TMSE} = \mathbb{E}[(\mathbf{s}_k(i) - \hat{\mathbf{s}}_k(i))^2]; \quad i = 1, 2, \ldots, n_s$$

where i denotes the ith element of $\mathbf{s}_k$ and $\hat{\mathbf{s}}_k$. TMSE(i) is obtained by reading the diagonal elements of updated $\mathbf{P}_k$.

For all scenarios, the $\mathbf{y}_k$ is assumed to available in spherical coordinate (as is the case in practice), i.e. $\mathbf{y}_k = [r_k, \theta_k, \phi_k]^T$. Consequently, the $\mathbf{h}(\mathbf{s}_k)$ is given by

$$\mathbf{h}(\mathbf{s}_k) = \left[\sqrt{x_k^2 + y_k^2 + z_k^2}, \tan^{-1}\left(\frac{y_k}{x_k}\right), \tan^{-1}\left(\frac{\sqrt{x_k^2 + y_k^2}}{z_k}\right) \right]^T.$$

Further, for all scenarios, we assume $\mathbf{Q}_s = \sigma_s^2 \mathbf{I}_{n_s}$ and $\mathbf{R}_m = \sigma_m^2 \mathbf{I}_{n_m}$, where σ_s and σ_m are chosen 0.01 and 0.25, respectively. For EKF-RKHS, the most commonly used Gaussian kernel with kernel width (σ) is used, i.e. $\kappa(\mathbf{s}_i, \mathbf{s}_j) = \exp\left(-\frac{\|\mathbf{s}_i - \mathbf{s}_j\|^2}{2\sigma^2}\right)$. In simulations, the λ and σ are chosen to obtain the optimum performance of EKF-RKHS. For all scenarios, λ and σ are fixed at 4×10^{-3} and 6, respectively. To simulate EKF and EKF-RKHS for indoor enviorment the target is assumed to move in 3D space along x, y, and z axis with the maximum distance of 10 m. Also, for scenario II and scenarios III, the maximum value of the target velocities v_{xk}, v_{yk}, and v_{zk} are limited to 2 m/sec and a_{xk}, a_{yk}, and a_{zk} are chosen form the bounded set $[-2, 2]$ m/sec^2. Further, in the following subsections, the simulation setup and the performance analysis of both EKF and EKF-RKHS for all scenarios are discussed in detail.

A. Constant displacement (scenario I)

For scenario I, the initial value of $\mathbf{s}_k$ i.e. $\mathbf{s}_0$ is chosen as $\mathbf{s}_0 = [x_0, y_0, z_0]^T$ and $\mathbf{s}_k$ is obtained by advancing $\mathbf{s}_{k-1}$ as

in (1) with $\Delta\mathbf{s} = [0.01\text{m}, 0.01\text{m}, 0.01\text{m}]^T$. The estimate $\hat{\mathbf{s}}_k$ is obtained at each kth time instance using EKF and EKF-RKHS. For both EKF and EKF-RMSE, TMSEs are obtained along x, y, and z axis.

The estimated trajectory using EKF and EKF-RKHS, the corresponding true trajectory (Ground truth), and measurements in rectangular coordinate are shown in Fig. 1. As shown in Fig. 1, the estimated trajectory obtained from EKF-RKHS has a closer proximity to Ground truth in comparison to trajectory estimated from EKF. The improved performance of EKF-RKHS is further shown in Fig. 2, which shows the TMSEs in estimatin of location in x, y and z axis. In Fig. 2, we observe that the TMSEs for EKF-RKHS is lower than the TMSEs for EKF, and that the TMSEs for EKF-RKHS and EKF converge at nearly identical time instances.
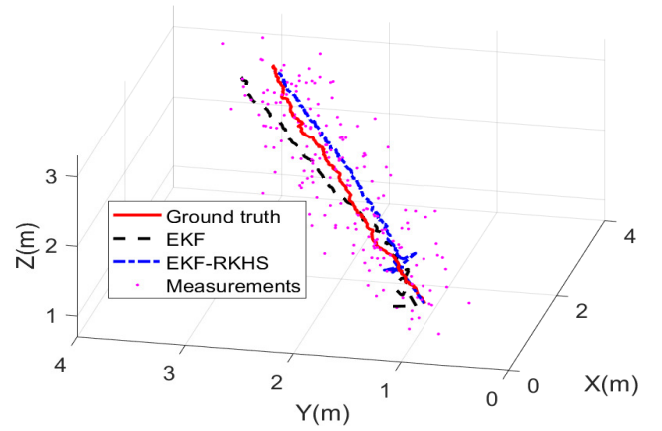

Fig. 1. Evolution of estimated trajectory in 3D space with EKF and EKF-RKHS for scenario I.
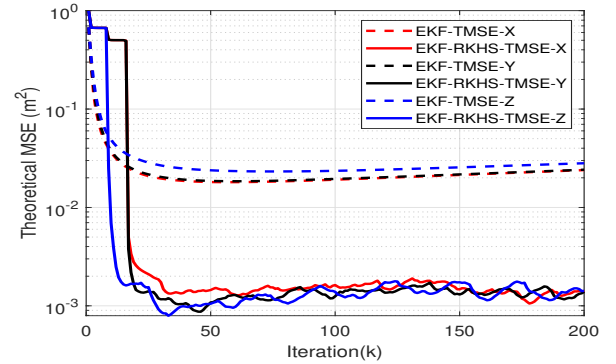

Fig. 2. Theoretical MSE along X, Y, and Z axis for EKF and EKF-RKHS and corresponding to scenario I.

B. Constant velocity (scenario II)

Here, $\mathbf{s}_0 = [1\text{m}, 2\text{m/sec}, 1\text{m}, 1\text{m/sec}, 1\text{m}, 0.5\text{m/sec}]^T$ and $\mathbf{s}_k$ is obtained from (2).

As shown in Fig. 3, the EKF-RKHS yields the estimated trajectory closer to the Ground truth. Further, Fig. 4 and Fig.

5 are respectively depicting the TMSEs for estimated locations and velocities along x, y, and z axis. From Fig. 4 and Fig. 5, it is explicit that, unlike scenario I, the TMSEs for EKF-RKHS are converging slower. However, for both locations and velocities, EKF-RKHS achieves lower TMSEs in the x, y, and z direction compared to EKF.
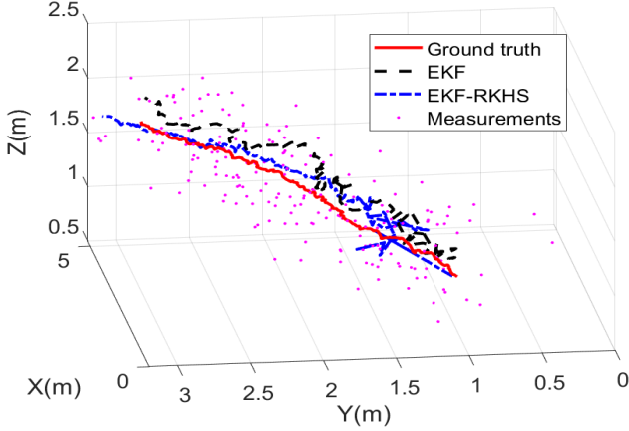

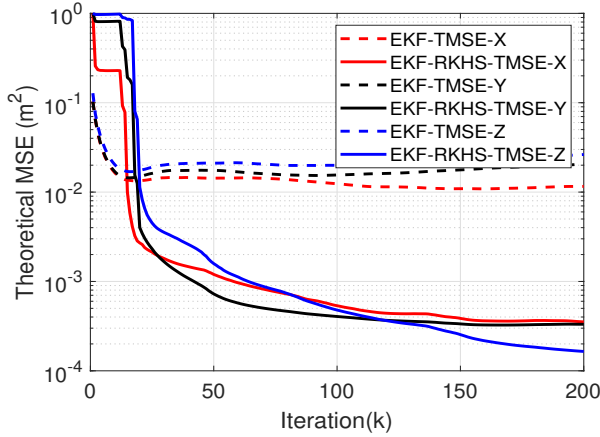Fig. 3. Evolution of estimated trajectory in 3D space with EKF and EKF-RKHS for scenario II.

Fig. 4. Theoretical MSE along X, Y, and Z axis for EKF and EKF-RKHS corresponding to scenario II.

C. Constant acceleration (scenario III)

Specific to scenario III, $\mathbf{s}_0 = [1\text{m}, 2\text{m/sec}, -2\text{m/sec}^2, 1\text{m}, 1.2\text{m/sec}, 2\text{m/sec}^2, 1\text{m}, 1.7\text{m/sec}, -1.5\text{m/sec}^2]^T$. Subsequently, $\mathbf{s}_k$ evolved using (3).

The comparative performance of EKF and EKF-RKHS are shown from Fig. 6 to Fig. 9 in terms of estimated trajectory and TMSEs. As depicted in Fig. 6, similar to the scenario I and II, the EKF-RKHS yield the estimated trajectory closer to the ground truth. Moreover, as shown in Fig. 7, unlike scenario I and scenario II, the TMSEs corresponding to location for both EKF-RKHS and EKF are not converging. However, the
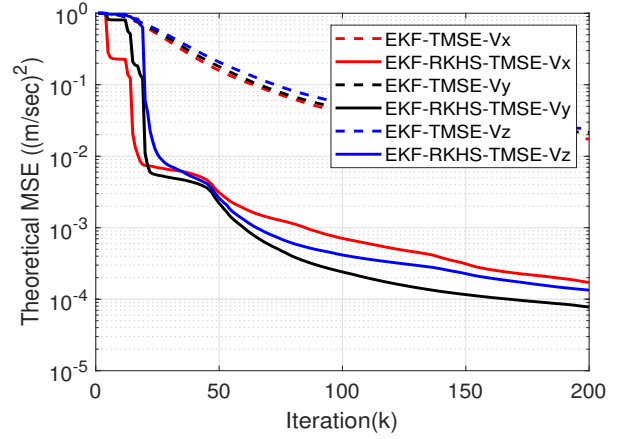

Fig. 5. Theoretical MSE for velocities in X, Y, and Z axis for EKF and EKF-RKHS corresponding to scenario II.
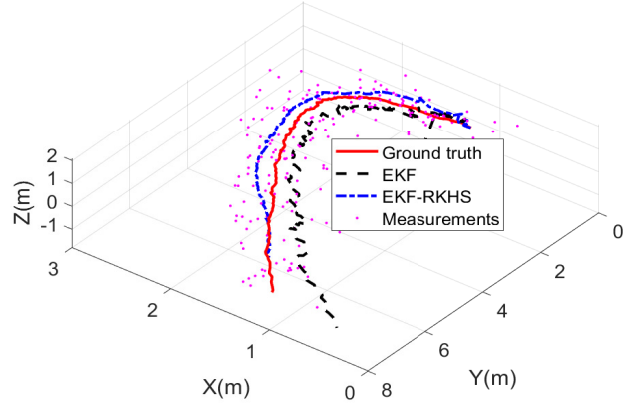

Fig. 6. Evolution of estimated trajectory in 3D space with EKF and EKF-RKHS for scenario III.

TMSEs for EKF-RKHS along the x and z axis are lower than the EKF. It is also observable that the TMSE for EKF-RKHS along the y axis is converging at a higher value than EKF. The observed behavior of EKF-RKHS along the y axis is because of the positive acceleration, which causes a fast movement along the y axis.

Further, Fig. 8 and Fig. 9, depicts that the TMSEs for velocities and accelerations are also lower for EKF-RKHS and nearly converging as well in comparison to TMSEs yield by EKF. Notably, as shown in Fig. 9, the TMSEs for accelerations along x, y, and z axis is not converging for EKF. On the contrary, EKF-RKHS yields acceleration TMSEs not only lower than EKF but also nearly converging. In one way, this validates the suitability of using EKF-RKHS for the scenario where the random target motion hinders the accurate estimation of the state vector.
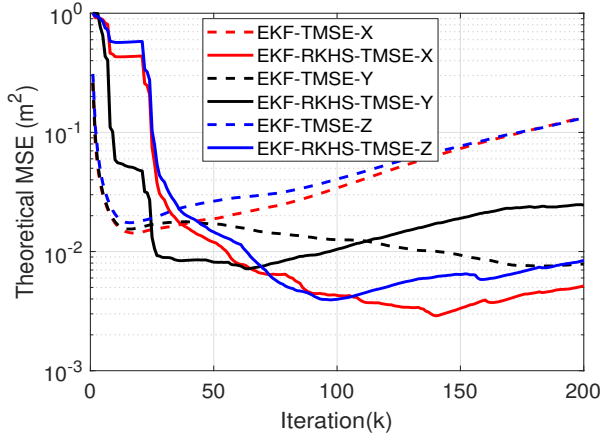
Fig. 7. Theoretical MSE for locations in X, Y, and Z axis for EKF and EKF-RKHS corresponding to scenario III.
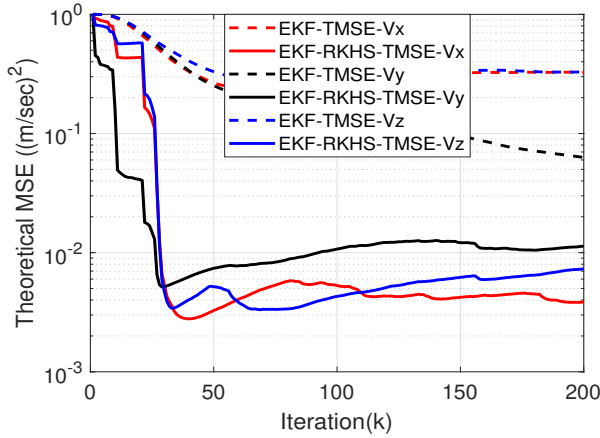

Fig. 8. Theoretical MSE for velocities in X, Y, and Z axis for EKF and EKF-RKHS corresponding to scenario III.
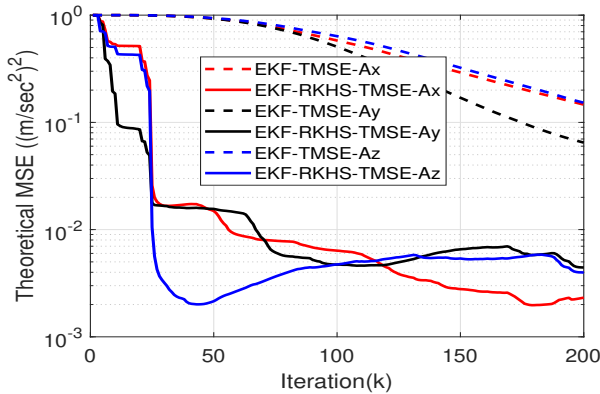

Fig. 9. Theoretical MSE for accelerations in X, Y, and Z axis for EKF and EKF-RKHS corresponding to scenario III.

V. CONCLUSIONS

Conventionally, EKF and UKF are used for the estimation of states hidden in a non-linear measurement. However, the ap-proximation of a non-linear measurement generally limits EKF and UKF to achieve high estimation accuracy. To overcome this shortcoming in EKF, the literature suggests replacing the approximation of the measurement function with its efficient estimate obtained in RKHS. Consequently, for the estimation of measurement function, RKHS based KRLS algorithm has been used; hence, the resulting filter is termed EKF-RKHS. In this paper, we have proposed to use EKF-RKHS for estimating the target's state vector moving in an indoor environment. In an indoor scene, the random motion hinders the accurate estimation of the state vector. The situation becomes more challenging when the measurements are available from the sensor in spherical coordinates. Therefore, with the help of three different motion models and using the measurements in spherical coordinates, we have proven the suitability of EKF-RKHS over EKF. Primarily, we have shown that in the case of the constant acceleration model, EKF-RKHS is the preferred choice over conventional EKF.

In the future, the extended KRLS algorithm can be used to estimate the measurement function. Also, the lower bound analysis of estimation accuracy achieved by RKHS based Kalman filter is the future scope of this work.

REFERENCES

[1] S. J. Julier and J. K. Uhlmann, "New extension of the Kalman filter to nonlinear systems," in *Signal Proces., sensor fusion, target recognition*, vol. 3068. Int. Soc. Optics Photon., 1997, pp. 182–194.

[2] ——, "Unscented filtering and nonlinear estimation," *Proceedings of the IEEE*, vol. 92, no. 3, pp. 401–422, 2004.

[3] M. A. Richards, *Fundamentals of radar signal processing*. Tata McGraw-Hill Education, 2005.

[4] S. S. Blackman, "Multiple-target tracking with radar applications," *Dedham*, 1986.

[5] W. Liu, J. C. Principe, and S. Haykin, *Kernel adaptive filtering: a comprehensive introduction*. John Wiley & Sons, 2011, vol. 57.

[6] U. K. Singh, R. Mitra, V. Bhatia, and A. K. Mishra, "Range and velocity estimation using kernel maximum correntropy based nonlinear estimators in non-Gaussian clutter," *IEEE Trans. Aerosp. and Electron. Sys.*, vol. 56, no. 3, pp. 1992–2004, 2020.

[7] W. Liu, P. P. Pokharel, and J. C. Principe, "The kernel least-mean-square algorithm," *IEEE Trans. Signal Process.*, vol. 56, no. 2, pp. 543–554, Jan. 2008.

[8] U. K. Singh, R. Mitra, V. Bhatia, and A. K. Mishra, "Kernel LMS-based estimation techniques for radar systems," *IEEE Trans. Aerosp. and Electron. Sys.*, vol. 55, no. 5, pp. 2501–2515, Oct 2019.

[9] P. Zhu, B. Chen, and J. C. Príncipe, "Learning nonlinear generative models of time series with a Kalman filter in RKHS," *IEEE Trans. Signal Process.*, vol. 62, no. 1, pp. 141–155, 2014.

[10] P. Zhu, B. Chen, and J. C. Príncipe, "Extended Kalman filter using a kernel recursive least squares observer," in *The 2011 International Joint Conference on Neural Networks*, 2011, pp. 1402–1408.

[11] F. Dinuzzo and B. Schölkopf, "The representer theorem for Hilbert spaces: a necessary and sufficient condition," *arXiv preprint arXiv:1205.1928*, 2012.

[12] Y. Engel, S. Mannor, and R. Meir, "The kernel recursive least-squares algorithm," *IEEE Trans. Signal Process.*, vol. 52, no. 8, pp. 2275–2285, 2004.